Thesis for the Degree of Master of Science

The effect of Fruits of *Hovenia dulcis* Thunb. on thermogenesis and its mechanism of action

Gahee Song

Department of Science in Korean Medicine

Graduate School

Kyung Hee University

Seoul, Korea

February, 2020

The effect of Fruits of *Hovenia dulcis* Thunb. on thermogenesis and its mechanism of action

Gahee Song

Department of Science in Korean Medicine

Graduate School

Kyung Hee University

Seoul, Korea

February, 2020

The effect of Fruits of *Hovenia dulcis* Thunb. on thermogenesis and its mechanism of action

By

Gahee Song

Advised by

Prof. Jae-Young Um, Ph.D.

Submitted to the Department of Science in Korean Medicine

and the Faculty of the Graduate School of

Kyung Hee University in partial fulfillment

of the requirements for the degree of

Master of Science

Dissertation Committee:

Chairman	Kwang Seok Ahn, Ph.D.
	Seong-Kyu Choe, Ph.D.
	Jae-Young Um, Ph.D.

Contents

I. Introduction.....1

II. Materials and Methods.....3

1. Chemical reagents and antibodies.....3
2. Preparation of the FHD extract.....3
3. Ethical statement.....4
4. Animal experiments.....4
5. Blood serum analysis.....4
6. Hematoxylin and eosin (H&E) staining.....5
7. Immunofluorescence (IF) assay.....5
8. Cell isolation, culture and adipocyte differentiation.....6
9. Cell cytotoxicity assay.....6
10. Oil Red-O staining.....7
11. RNA isolation and real-time RT-PCR.....7
12. Protein extraction and western blot analysis 9
13. Mitochondrial microscopic analysis 9
14. DNA isolation and Mitochondria DNA (mtDNA) copy number assay 9
15. Total intracellular NAD assay.....10
16. Oxygen consumption analysis.....10
17. Statistical analysis.....10

III. Results.....11

1. FHD decreases body weight and lipid size of BAT in HFD-induced obese C57BL/6 mice 11

2. FHD upregulates thermogenesis-related factors in BAT of HFD-induced obese C57BL/6 mice and primary cultured brown adipocyte……..……..13
3. FHD increases mitochondria-related factors in BAT of HFD-induced obese C57BL/6 mice and primary cultured brown adipocyte ……..…..17
4. FHD increases SIRT family in BAT of HFD-induced obese C57BL/6 mice and primary cultured brown adipocytes ……..…22

IV. Discussion.....24

V. Conclusion.....29

VI. References.....30

국문초록.....35

List of Tables

Table 1. primer sequences used for real-time RT-PCR.....8

List of Figures

Figure 1. FHD decreases body weight and lipid diameter size in HFD-induced obese C57BL/6 mice……12

Figure 2. FHD upregulates expressions of thermogenic factors in BAT of HFD-induced obese C57BL/6 mice……14

Figure 3. FHD stimulates brown adipocyte differentiation in primary cultured brown adipocyte……15

Figure 4. FHD increases thermogenic factors in primary cultured brown adipocyte……16

Figure 5. FHD increases mitochondria related factors in BAT of HFD-induced obese C57BL/6 mice ……19

Figure 6. FHD increases mitochondria number in primary cultured brown adipocyte……..……20

Figure 7. FHD activates mitochondria biogenesis in primary cultured brown adipocyte……21

Figure 8. FHD activates SIRT family in BAT of of HFD-induced obese C57BL/6 mice and primary cultured brown adipocyte…… ..……23

Figure 9. Diagrammatic visualization showing the contribution of FHD to the pharmacological pathways of obesity……..28

Abbreviations

ALT, alanine transaminase;

AST, aspartate aminotransferase;

BAT, brown adipose tissue;

CYT C, Cytochrome C;

DM, differentiation medium

FHD, Fruits of *Hovenia dulcis* Thunb.;

FIS1, mitochondrial fission 1;

GAPDH, glyceraldehyde-3-phosphate dehydrogenase;

H&E, hematoxylin and eosin;

HFD, high-fat diet;

LDL-C, low-density lipoprotein cholesterol;

MFN1, mitofusin 1;

ND, normal diet;

NRF, nuclear respiratory factor;

OXPHOS, oxidative phosphorylation system;

PGC1α, peroxisome proliferator activated receptor gamma-coactivator 1 alpha;

PRDM16, PR domain containing 16

SIRT, sirtuin

TC, total cholesterol;

TOM20, mitochondrial preprotein translocases of the outer membrane 20

UCP1, uncoupling protein 1;

ABSTRACT

The effect of the Fruits of *Hovenia dulcis* Thunb. on thermogenesis and its mechanism of action

By Gahee Song

Advised by Prof. Jae-Young Um

Adipocytes are divided into two types, brown and white adipocytes, which have opposing functions. White adipocyte is responsible for the occurrence of obesity as it stores energy as lipid. On the other hand, brown adipocytes, which contain abundant mitochondria, use stored energy as fuel during a process called non-shivering thermogenesis. Thus, the pharmacological activation of non-shivering thermogenesis in brown adipocytes has risen into a promising target for treating obesity. This study attempted to investigate the role of fruit of *Hovenial dulcis* Thunb. (FHD), a frequently used herbal treatment for liver diseases, on thermogenesis and its mechanism using primary cultured brown adipocytes and BAT of HFD-induced obese mice. Thermogenesis-related factors including uncoupling protein 1 and peroxisome proliferative activated receptor gamma coactivator 1 alpha were increased by FHD treatment. FHD also increased mitochondrial biogenesis and activation factors such as sirtuin 3 and sirtuin 1 as well as nuclear respiratory factor 1 and oxidative phosphorylation protein complex. Furthermore, FHD increased intracellular NAD+ level, which may possibly be responsible for the activation of the thermogenic reaction. These results indicate that FHD can be a potential substance for improving obesity due to its thermogenic action through mitochondrial biogenesis and activation.

Keywords: Fruit of *Hoveina dulcis* Thunb.; obesity; brown adipocyte; thermogenesis; mitochondria

I. INTRODUCTION

Brown adipose tissue (BAT) was identified in adult humans using fluorodeoxyglucose positron emission tomography [1]. The fact that the thermogenic activity of the BAT has been shown to be reduced according to age and BMI [1]. Moreover, it has been demonstrated that the tissue can be activated in response to multiple stimuli, such as cold exposure, insulin, and beta3-adrenergic receptor agonist [2-4]. These observations inspired researchers to study BAT as a potential new target for obesity treatment

Adipose tissue can be categorized into brown and white adipose tissue. White adipose tissue (WAT) is a storage place, playing a role in accumulating lipid. Excessive lipid accumulation is known as a major cause of coronary cardiovascular diseases, obesity, hyperlipidemia, and hypertension [5, 6]. In contrast, BAT possess abundant mitochondria with numerous multi-locular lipid droplets, and plays a crucial role in using stored lipid by dissipating heat: a process called non-shivering thermogenesis [7]. Thus, BAT can regulate body weight, lipid metabolism, and body temperature: the whole-body energy metabolism [8]. BAT is found only in mammals and is present at birth. It is at its highest levels in early life, and decreases with age in humans [9]. The amount of BAT in adult humans has been reported to be highly correlated with their degree of obesity, indicating that BAT may play an important role in the prevention and treatment of obesity [10]. Therefore, BAT stimulation via mitochondrial activation can be a key target to improve obesity.

The mitochondria of BAT is equipped with a specialized protein known as uncoupling protein 1 (UCP1), which short-circuits the electron transport chain allowing the mitochondrial membrane potential to be transduced to heat instead of ATP production [11]. The BAT is capable of altering the energy expenditure and metabolism in mammals without increasing physical activity due to its abundant mitochondria, which regulates cell metabolism [12]. Mitochondrial metabolic processes of adipose tissue are largely dependent on the NAD+ homeostasis. The mitochondrial dysfunction by disrupted NAD homeostasis has been suggested to be one of the major causes for obesity and metabolic complications [13]. Mitochondrial metabolism can be regulated by NAD-dependent

enzymes, sirtuins (SIRTs) and poly ADP-ribose polymerases, which have opposing effects [14, 15]. Among them, SIRT1 is an ortholog of nuclear NAD+ dependent protein deacetylase. SIRT1 activation is closely controlled by different environments that can change the cellular NAD+ availability. For example, a high-energy state that decreases cellular NAD+ levels, including feeding a high-fat diet and acute inflammatory responses, reduces SIRT1 activity [16]. Therefore, SIRT1 in particular is an important regulator of various cellular processes, from energy metabolism and stress response [17].

Hovenia dulcis Thunb., a member of Rhamnaceae, is mainly found in Korea, China, India, and Japan. The fruits, seeds, leaves, roots, and bark of this tree are used in traditional Korean medicine for various purposes including inflammation and liver diseases. Among the parts of *Hovenia dulcis* Thunb., the fruits of *Hovenia dulcis* Thunb. (FHD) contain an extensive variety of pharmaceutically active compounds, such as ampelopsin, taxifolin, myricetin and quercetin [18]. Ji et al. report its beneficial effect on diabetes by reducing blood sugar and hepatic glycogen [19]. A previous study by Kim and colleauges also investigated and reported the effect of FHD on the adipogenesis in 3T3-L1 adipocytes. As a result, FHD modulated adipogenic fators such as the peroxisome proliferator-activated receptor-γ and CCAAT/enhancer-binding protein-α through AMP-activated protein kinase (AMPK)-α [19]. However, its thermogenic action and the underlying mechanism is not verified to date. In this study, the author studied whether FHD can activate the non-shivering thermogenesis pathway using BAT of high fat diet (HFD)-induced obese C57BL6 mice and primary cultured brown adipocytes.

II. MATERIALS AND METHODS

1. Chemical reagents and antibodies

Dulbecco's modified Eagle's medium (DMEM), penicillin– streptomycin-glutamine, and fetal bovine serum (FBS) were purchased from Gibco BRL (NY, USA). Insulin, 3-isobutylmethylxanthine (IBMX), dexamethasone (DEX), and Oil-Red-O powder were purchased from Sigma Chemical Co. (MO, USA). Olaparib (10621) and NAD+ (16077) were purchased from Cayman Chemical Company (MI, USA). Antibodies for SIRT3 (5490S), UCP1 (14670S), NRF2 (12721), NRF1 (12381), and Cytochrome C (CytC) (4272) and were purchased from Cell Signaling Technology (MA, USA); antibodies for glyceraldehyde-3-phosphate dehydrogenase (GAPDH) (sc-32233), mitochondrial preprotein translocases of the outer membrane 20 (TOM20) (sc-17764), mitochondrial fission 1 (FIS1) (sc-376447), and mitofusin-1 (MFN1) (sc-166644) antibody was purchased from Santa Cruz Biotechnology (CA, USA); antibodies for PGC1α (ab54481), PR domain containing 16 (PRDM16) (ab106410), Total OXPHOS (ab110413) were purchased from Abcam (Cambridge, UK).

2. Preparation of the FHD extract

The water extract of FHD were provided by SEROM Co., Ltd (Jangheung, South Korea). Briefly, 100 g of FHD in 1 L of water was boiled over 95℃ for 8 h and the residue was boiled over 95℃ for another 8 h with additional 500 ml of water. Then the residue was filtered, lyophilized, and kept at −20℃. The yield was 6%. Dilutions were made in saline and filtered through a 0.22 μm syringe filter. A previous study by Kim and colleauges, the phytochemical profile of FHD using HPLC and GC-MS analysis was investigated and identified compounds of 2,3-dihydro-3,5-dihydroxy-6-methyl-4(H)-pyran-4- one, 5-hydroxymethyl-2-furancarboxaldehyde, and quercetin [20].

3. Ethical statement

All animal experiments were performed according to the Guide for the Care and Use of Laboratory Animals and were approved by the Institutional Review Board of Kyung Hee University (confirmation number: KHUASP (SE)-13-012).

4 Animal experiments

Male C57BL/6J mice (4 weeks old) were purchased from Daehan Biolink (Eumsung, South Korea) and maintained for 1 week before the experiments. To induce obesity in the mice, they were fed a high-fat diet (HFD; rodent diet D12492; Research Diet, NJ, USA) consisting of 60% fat for 4 weeks before administrating FHD (5 mg/kg/day). The mice were then randomly divided into two groups (n = 6/group): HFD and HFD with 5 mg/kg/day FHD. An additional 7 weeks administration experiment was done with these groups and a normal control group, with the latter fed a normal diet (ND).

Body weight and food intake of the mice were measured once a week. At the end of the experiment, the animals were anesthetized under CO^2 asphyxiation, and serum was separated immediately after blood collection via cardiac puncture. The tissues were collected and stored at -80℃.

5. Blood serum analysis

Serum creatinine, total cholesterol (TC), low-density lipoprotein-cholesterol (LDL-C), high-density lipoprotein-cholesterol (HDL-C), alanine transaminase (ALT), aspartate aminotransferase (AST), and glucose were analyzed using enzymatic colorimetric methods by Seoul Medical Science Institute (Seoul Clinical Laboratories, Seoul, South Korea).

6. Hematoxylin and eosin (H&E) staining

Hematoxylin and eosin (H&E) staining was done as previously described [20]. Brielfly, the BAT were collected, washed in saline and fixed in 10% formaldehyde, and then dehydrated using grades 70%, 80%, 90%, 95%, and 100% ethanol. After clearing in a change of xylene, the samples were impregnated with molten paraffin wax, then embedded and blocked out. The tissues were then cut into 4.5 μm sections and stained with hematoxylin and eosin. Photographs were taken under a microscope EVOS M7000 (Thermo Fisher Scientific, MA, USA). The average adipocyte cell size and the number of cells were measured using the NIH Image J software program (National Institute of Health, MD, USA).

7. Immunofluorescence (IF) assay

The cells and tissues were fixed using 10% formalin and blocked with 5% BSA for 1 h. After the cells and tissue were incubated with the indicated primary antibodies (anti-UCP1/2/3, anti-PGC1α, anti-TOM20, anti-MFN1, and anti-FIS1, 1:50-200 in 5% BSA) overnight at 4℃, the cells and tissue were washed and then incubated with Alexa Flour 488- or 633-conjugated secondary antibody (1:1000), and the fluorescence was detected using an EVOS M7000 (Thermo Fisher Scientific, MA, USA).

8. Cell isolation, culture, and adipocyte differentiation

Brown pre-adipocytes primary cultured brown adipocytes isolation, culture, and differentiation were performed as previously described [22]. Briefly, after sacrificed by decapitation under CO^2 asphyxiation, interscapular BAT was isolated from newborn FVB mice (Daehan Biolink Co., Eumsung, South Korea), minced, and subjected to collagenase digestion (10 mg of collagenase in 10 ml of isolation buffer containing 0.123 M NaCl, 5 mM KCl, 1.3 mM CaCl2, 5 mM glucose, 100 mM Hepes, and 4% BSA) for 1 h. The digested tissue was filtered through a 100 μm nylon filter. The collected cells were centrifuged (200 × g) for 5 min. Cells were resuspended in 10 ml of culture medium (DMEM containing 25 mM glucose, 20% FBS, 20 mM Hepes), seeded on 100 mm plates, and grown at 37°C in a humidified atmosphere of 5% CO^2 and 95% air. Primary brown pre-adipocytes were induced to differentiate into mature brown adipocytes, on day 2 after confluence (Day 0), cells were placed in a differentiation medium consisting of DMEM, 10% FBS, and a differentiation media (DM) (0.5 mM IBMX, 0.5 μM DEX, 20 nM insulin, 125 mM indomethacin, and 1 nM 3,3′,5-triiodo-L-thyronine [T3]). On day 4, they were then switched to a maintenance medium composed of DMEM, 10% FBS, 1 nM T3, and 20 nM insulin. The medium was replenished every 2 days. Full differentiation of the cells was achieved on Day 8. On Day 2, FHD was prepared in a differentiation medium at concentrations of 10 μg/ml and 100 μg/ml.

9. Cell cytotoxicity assay

Cell viability was measured with a Cell Proliferation MTS kit (Promega Co., WI, USA) as previously described [22]. Briefly, Cells were seeded (2×10^4 cells per well) on 96-well plates and incubated for 24 h, followed by incubation with various concentrations (10, 100, 500 and 1000 μg/ml in primary cultured brown adipocytes) of FHD in culture medium for an additional 48 h. The absorbance was measured at 490 nm in a VERSAmax microplate reader (Molecular Devices, CA, USA).

10. Oil Red O staining

Intracellular TG accumulation was measured using the Oil Red-O staining method as previously described [20]. Photomicrograph images were obtained from a regular light microscope (Olympus, Tokyo, Japan), and absorbance was measured at 500 nm using a VERSAmax microplate reader (Molecular Devices, CA, USA).

11. RNA isolation and real-time RT-PCR

Total RNA was extracted using a GeneAllR RiboEx Total RNA extraction kit (GeneAll Biotechnology, Seoul, South Korea). RNA (2 μg) was used as a template for first-strand cDNA synthesis performed using a Maxime RT PreMix (INTRON Biotechnology, Seoul, Korea) according to the manufacturer's instructions. Newly synthesized cDNA from FHD-treated brown adipocytes was amplified using specific primers and the Fast SYBR Green PCR Master Mix (Applied Biosystems, Foster City, CA, USA). The PCR process was carried out for 40 cycles at 95°C for 15 s and 60°C for 1 min. PCR products were measured with a StepOnePlus real-time RT-PCR System, and the relative gene expressions were calculated based on the comparative CT method using the StepOne Software v2.1 (Applied Biosystems, CA, USA). The primers used in the experiments are shown in Table 1.

Table1. primer sequences used for real-time RT-PCR

Genes	5' to 3' oligonucleotide sequences
Mouse *Ucp1*	
Sense (forward)	AGGCTTCCAGTACCATTAGGT
Antisense (reverse)	CTGAGTGAGGCAAAGCTGATTT
Mouse *Ppargc1a*	
Sense (forward)	TTCATCTGAGTATGGAGTCGCT
Antisense (reverse)	GGGGGTGAAACCACTTTTGTAA
Mouse *Sirt3*	
Sense (forward)	ATCCCGGACTTCAGATCCCC
Antisense (reverse)	CAACATGAAAAAGGGCTTGGG
Mouse *Prdm16*	
Sense (forward)	CCAAGGCAAGGGCGAAGAA
Antisense (reverse)	AGTCTGGTGGGATTGGAATGT
Mouse *Cox4*	
Sense (forward)	ATTGGCAAGAGAGCCATTTCTAC
Antisense (reverse)	CACGCCGATCAGCGTAAGT
Mouse *Cox8*	
Sense (forward)	TGTGGGGATCTCAGCCATAGT
Antisense (reverse)	AGTGGGCTAAGACCCATCCTG
Mouse *Nrf1*	
Sense (forward)	CCACGTTGGATGAGTACACG
Antisense (reverse)	CAGACTCGAGGTCTTCCAGG
Mouse *Cidea*	
Sense (forward)	TGACATTCATGGGATTGCAGAC
Antisense (reverse)	GGCCAGTTGTGATGACTAAGAC
Mouse *Cycs*	
Sense (forward)	CCAAATCTCCACGGTCTGTTC
Antisense (reverse)	ATCAGGGTATCCTCTCCCCAG
Mouse *Dnm1l*	
Sense (forward)	CAGGAATTGTTACGGTTCCCTAA
Antisense (reverse)	CCTGAATTAACTTGTCCCGTGA
Mouse *Mfn1*	
Sense (forward)	ATGGCAGAAACGGTATCTCCA
Antisense (reverse)	CTCGGATGCTATTCGATCAAGTT
Mouse *Gapdh*	
Sense (forward)	AGGTCGGTGTGAACGGATTTG
Antisense (reverse)	TGTAGACCATGTAGTTGAGGTCA

Ucp1 : uncoupling protein 1, *Ppargc1a* : peroxisome proliferative activated receptor, gamma, coactivator 1 alpha, *Sirt3* : sirtuin 3, *Prdm16* : PR domain containing 16, *Cox4* : cytochrome c oxidase subunit 4I1, *Cox8* : cytochrome c oxidase subunit 8b, *Nrf1* : nuclear respiratory factor 1, *Cidea* : cell death-inducing DNA fragmentation factor, alpha subunit-like effector A, *Cycs* : cytochrome c, *Dnm1l* : dynamin 1-like, *Mfn1* : mitofusin 1, *Gapdh* : glyceraldehyde-3-phosphate dehydrogenase-

12. Protein extraction and western blot analysis

Western blot analyses were performed as previously described [20]. In brief, homogenized tissues or harvested cells were lysed in lysis buffer (Cell Signaling Technology, MA, USA), and protein concentration was determined using a protein assay reagent (Bio-Rad Laboratories, CA, USA). Equal amounts of total protein were resolved by 10–15% sodium dodecyl sulfate-polyacrylamide gel electrophoresis and transferred to a polyvinylidene difluoride membrane. The membranes were incubated with the primary antibody at 4℃ over-night, and then incubated with a 1:10000 dilution of the proper horseradish peroxidase (HRP)-conjugated secondary antibody (Jackson Immuno Research, PA, USA) for 1 h at room temperature.

13. Mitochondrial microscopic analysis

To label the mitochondria, the cells were incubated with Mito-Tracker Red CMXRos (Molecular Probes, OR, USA). The cells were fixed and permeabilized, after which a prewarmed (37 ℃) staining solution containing Mito-Tracker probes 200nmol/l was applied. The cells were incubated in this solution for 30 min. After the staining was complete, the solution was replaced with fresh prewarmed (37 ℃) media. Fluorescent signals were imaged with IX71 fluorescence microscope (Olympus, Tokyo, Japan) as previously described [22].

14. DNA isolation and mitochondria DNA (mtDNA) copy number assay

Whole genomic DNA from primary cultured brown adipocytes were isolated using AccuPrep® Genomic DNA Extraction kit (Bioneer, Deajeon, South Korea) according to the manufacturer's protocol. DNA was quantified using a Nanodrop 2000 Spectrometry (Thermo Fisher Scientific, MA, USA). Whole cell genomic DNA was used to assess mtDNA copy number by RT-PCR using the Mouse mtDNA Copy Number Kit (MCN2) from Detroit R&D, Inc (Detroit, MI, USA).

15. Total intracellular NAD assay

The harvested cells were lysed with 400 μl of NADH/NAD Extraction Buffer and centrifuged for 10 min at 4 °C at 10,000 × g. The supernatant was centrifuged at 10,000 × g for 20 min at 4 °C. The filtrate was collected and used for NAD assay via the NAD/NADH Assay Kit (Abcam, Cambridge, UK) according to the manufacture's protocol. The measured values were normalized to lysate protein levels. The absorbance was measured at 450 nm in a VERSAmax microplate reader (Molecular Devices, CA, USA).

16. Oxygen consumption analysis

Real time oxygen consumption in the harvested cells were measured by Mito-ID Extracellular O_2 sensor kit (Enzo Life Science, Lausen, Switzerland) according to the instruction provided Enzo Life Science. Briefly, Primary cultured brown adipocyte cultured and differentiate previously same thing. When full differentiation of the cells was achieved on Day 8 the media was changed with 150 μl of DMEM with 10% FBS. And O_2 sensor probe (10 μl) was added into each well. After covering with 2 drops (about 100 μl) of Mito-ID HS Oil, the plates were read of 380 nm for excitation and 650 nm of emission at 30 °C. Normalization of the measured values is done by the cell number by DAPI. The absorbance was measured in a VARIOSKAN LUX spectrophotometer (Thermo Fisher Scientific, MA, USA).

17. Statistical analysis

Data were expressed as the means ± standard error mean (S.E.M.). Significant differences ($p < 0.05$) between groups were determined using a *t*-test. All statistical analyzes were performed using an SPSS statistical analysis software version 11.5 (SPSS Inc., IL, USA).

III. RESULTS

1. FHD decreases body weight and lipid size of BAT in HFD-induced obese C57BL/6 mice

To investigate whether FHD regulates body weight gain, mice were fed a HFD for 4 weeks before administrating FHD. After inducing obesity, the mice were subdivided into two groups (n = 6/group): a HFD group and a HFD group with FHD (5 mg/kg/day) treatment. These groups had similar body weight at the beginning of the study. The mice fed a HFD diet gained significantly more body weight than those fed a normal diet. However, in the FHD treatment group the mice showed significantly reduced body weight of 8.88% than the HFD-fed group (Fig. 1A). Food intake was the same for all groups (Fig. 1B). After 12 weeks of experiment, a plasma parameter analysis was conducted. Serum TC, LDL-C, HDL-C, glucose, ALT, AST, and creatinine were measured. Serum creatinine level remained unchanged in FHD-fed mice (Fig. 1C). The FHD-fed group showed lower numbers in the levels of glucose and TC compared to the HFD-fed mice, but without statistical significance (Fig. 1D). In addition, FHD raised the level of HDL-C (Fig. 1D). The serum levels of ALT, AST and creatinine was relatively lower in FHD-fed mice ($p > 0.05$) (Fig. 1E). From H&E staining of BAT, the size of lipid droplets was decreased by FHD treatment (Fig. 1F-G).

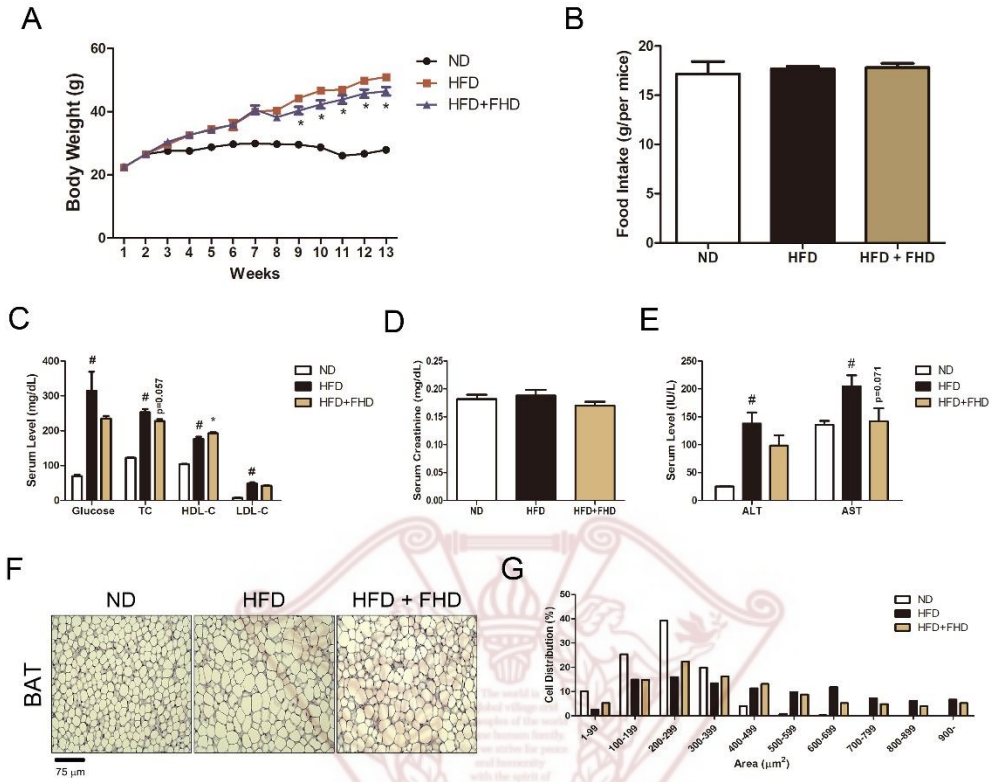

Figure 1. FHD decreases body weight and lipid diameter sizes in HFD-induced obese C57BL/6 mice.

Mice were administered FHD (5 mg/kg per day) for 7 weeks. (A) Changes in body weight were measured. (B) Food intake was measured. Serum levels of (C) glucose, TC, HDL-C, LDL-C, (D) creatinine, (E) ALT, and AST levels were measured. (F) Paraffin-embedded BAT sections from ND, HFD, and FHD mice were stained with H&E (original magnification, ×400). (F) Lipid diameters were measured the percentages of different size lipids calculated and plotted. All values are mean ± S.E.M. of data from three separate experiments. $^{\#}$ $p < 0.05$ vs ND-fed mice; $^{*}p < 0.05$ vs HFD-fed mice. BAT, brown adipose tissue; HFD, high-fat diet; ND, normal diet.

2. FHD upregulates thermogenesis-related factors in BAT of HFD-induced obese C57BL/6 mice and primary cultured brown adipocyte

A major tissue of non-shivering thermogenesis is BAT, in which heat is produced by UCP1 [23]. Thus, the author investigated whether FHD can induce thermogenesis-related factors in BAT. The protein expressions of PGC1α and UCP1, which are the specific markers of thermogenesis, were significantly increased in BAT of the FHD-fed group compared to the HFD-fed group. (Fig. 2A). IF analyses showed the increased expression of UCP1/2/3 and PGC1α in BAT of FHD-fed mice as seen in Fig 2B.

To investigate the related mechanisms of the thermogenic effect of FHD, *in vitro* studies using primary cultured brown adipocytes were carried out. First, to confirm the cytotoxicity of FHD in primary cultured brown adipocytes, the cells were treated with various concentrations (0–1000 μg/ml) of FHD, and an MTS assay was performed. Treatment with 10 and 100 μg/ml of FHD did not display any cytotoxicity in primary cultured brown adipocytes (Fig. 3A), thus these two concentrations were chosen for further experiments. Next, to determine the effects of FHD on brown adipocyte differentiation, lipid accumulation was measured by Oil Red O staining after FHD treatment. As a result, lipid accumulation was significantly increased by FHD (10 and 100 μg/ml) in brown adipocytes (Fig. 3B) IF analyses of UCP1 and PGC1α, the specific markers of thermogenesis, were also increased by FHD treatment, locating in the cytoplasm of primary cultured brown adipocytes, consistent to the *in vivo* results (Fig. 4A). Real-time RT-PCR results showed significantly enhanced levels of thermogenesis-related genes including *Ucp1, Ppargc1a,* and *Prdm16* in FHD-treated cells (Fig. 2F). The protein expressions of PRDM16, PGC1α, and UCP1 in brown adipocytes were significantly upregulated by FHD as well (Fig. 4B). The protein expressions of PRDM16, PGC1α, and UCP1 in brown adipocytes were significantly upregulated by FHD as well (Fig. 4C). These results suggest that FHD can activate thermogenesis-related factors *in vivo* and *in vitro*.

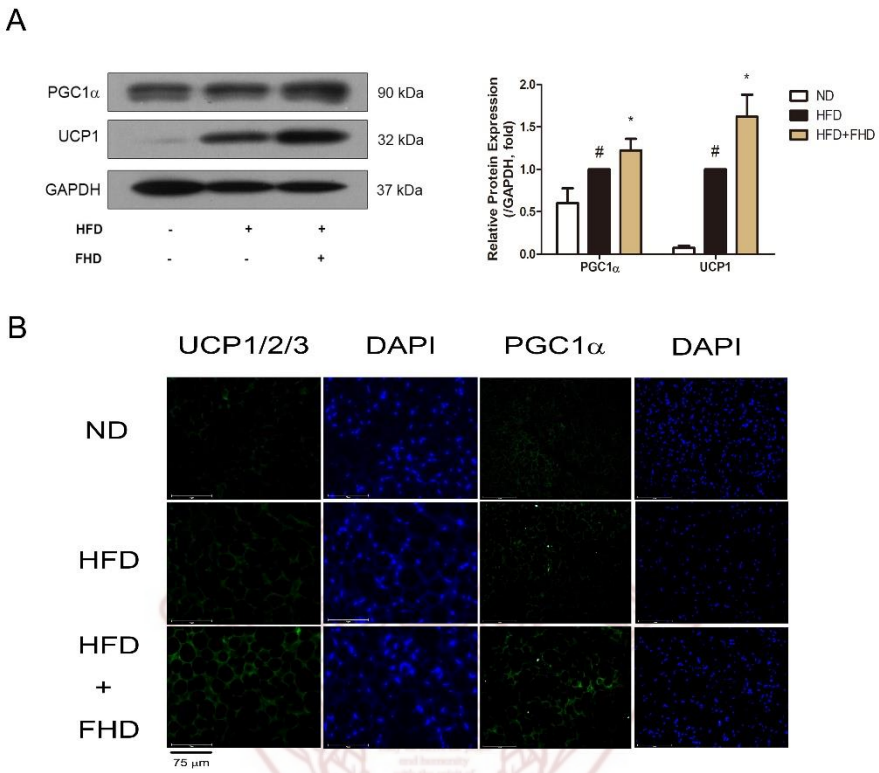

Figure 2. FHD upregulates expressions of thermogenic factors in BAT of HFD-induced obese C57BL/6 mice.

(A) Protein levels of UCP1 and PGC1α were analyzed by a Western blot analysis. (B) Paraffin-embedded BAT sections from ND, HFD, and HFD+FHD mice were immunostained with antibodies for UCP1/2/3 and PGC1α, and counter-stained with DAPI for visualization of cell nucleus (original magnification, ×400). Results were expressed relative to GAPDH. All values are the means ± S.E.M. of three independent experiments. $^{\#}p < 0.05$, vs. ND-fed mice; $^{*}p < 0.05$, vs. HFD-fed mice. BAT, brown adipose tissue; HFD, high-fat diet; ND, normal diet.

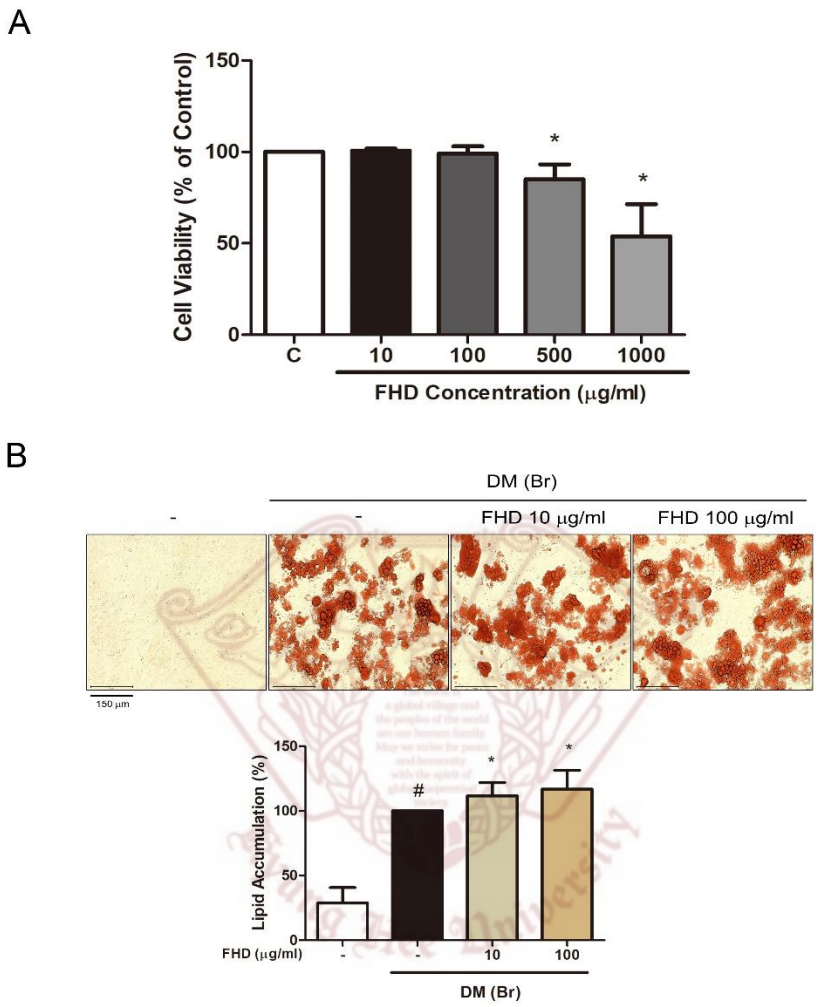

Figure 3. FHD stimulates brown adipocyte differentiation in primary cultured brown adipocyte.

(A) Primary cultured brown adipocytes were incubated with FHD at the indicated concentrations (10, 100, 500, and 1000 μg/ml) for 48 h and Cell viability was assessed by the MTS assay. (B) Primary brown cultured adipocytes were differentiated in the absence or presence of FHD (10 and 100 μg/ml). Lipid droplets were measured by Oil Red O staining (original magnification, ×200). All values are the means ± S.E.M. of three independent experiments. $^{\#}p < 0.05$, vs. DM-undifferentiated control cells; $^{*}p < 0.05$, vs. DM-differentiated control cells. DM, differentiated medium.

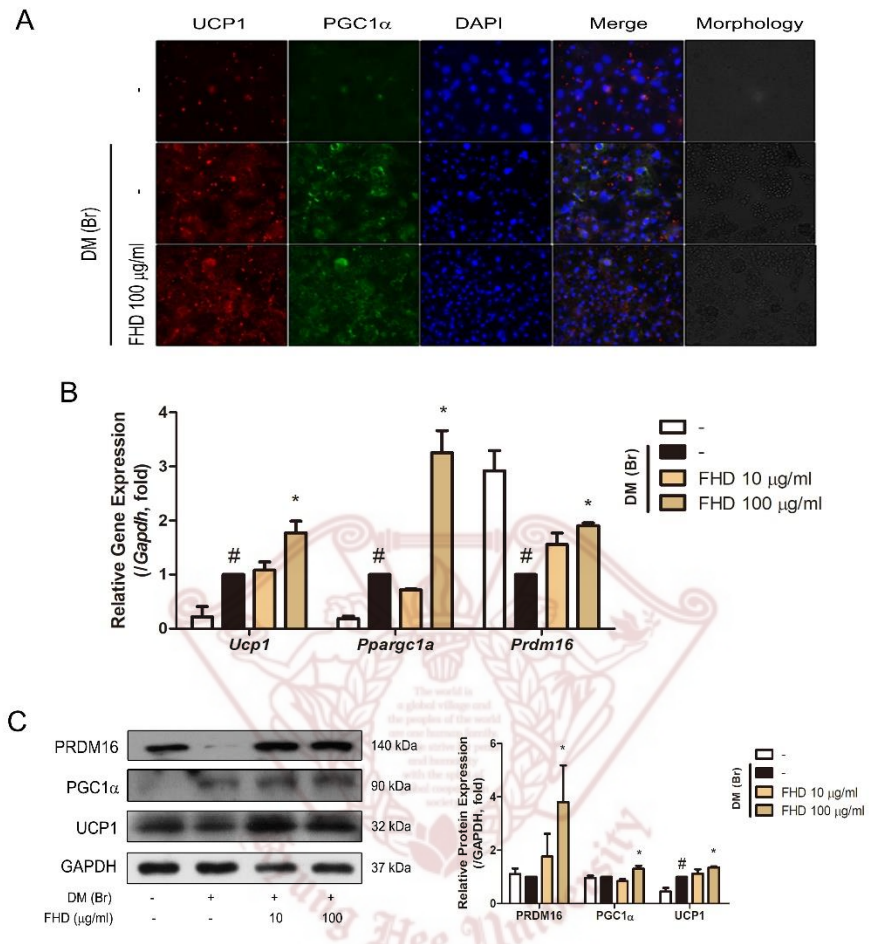

Figure 4. FHD increases thermogenic factors in primary cultured brown adipocyte.
(A) Primary cultured brown adipocytes were immunostained with antibodies for UCP1 and PGC1α, and counter-stained with DAPI for visualization of cell nucleus. (B) The mRNA of *Ucp1*, *Ppargc1a*, and *Prdm16* were analyzed by real-time RT-PCR. (C) Protein levels of UCP1, PGC1α, and PRDM16 were analyzed by a Western blot analysis. Results were expressed relative to GAPDH. All values are the means ± S.E.M. of three independent experiments. $^{\#}p < 0.05$, vs. DM-undifferentiated control cells; $^{*}p < 0.05$, vs. DM-differentiated control cells. DM, differentiated medium.

3. FHD increases mitochondria-related factors in BAT of HFD-induced obese C57BL/6 mice and primary cultured brown adipocyte

Thermogenic activation of brown adipocytes is highly dependent on mitochondrial biogenesis [7]. Therefore, the author investigated whether FHD can activate mitochondria in BAT of HFD-fed obese mice and primary cultured brown adipocytes. First, mitochondria-related factors by FHD were determined in BAT. First, mitochondria-related factors by FHD were determined in BAT. The HFD-fed mice with FHD treatment showed increased protein expression levels of NRF1 and MFN1, which are both involved in mitochondrial biogenesis (Fig. 5A). As seen in Fig. 3B, IF staining of mitochondria-associated markers such as MFN1, FIS1 and TOM20 in BAT also verified the action of FHD. The mitochondrial OXPHOS complex which participates in mitochondria beta-oxidation and biogenesis were also examined in BAT. FHD treatment significantly increased the expression protein levels of complex 1, 2, 4 (Fig. 5C). These results indicate that FHD treatment increased energy expenditure through the modulation of mitochondrial biogenesis and beta-oxidation in BAT.

To confirm the effects of FHD on mitochondria biogenesis of brown adipocytes, the author performed additional assays of mito-tracker staining and mtDNA copy numbers to identify the abundance of mitochondria in primary cultured brown adipocytes. FHD treatment in primary cultured brown adipocytes showed increased mitochondria numbers when compared to vehicle-treated adipocytes (Fig. 6A-B). In addition, the level of mitochondria biogenesis-related genes was measured by real-time RT- PCR. The mRNA levels of *Cox4, Cox8, Nrf1, Cidea, Mfn1, Dnm1l* and *Cycs* were significantly increased in a dose-dependent manner by FHD treatment (Fig. 7A). In line, the protein levels of NRF2, MFN1, NRF1, and CytC were increased by FHD as well (Fig. 7B). Furthermore, when the oxygen consumption was investigated in FHD-treated brown adipocytes, it was confirmed that the oxygen consumption in primary brown adipocytes was significantly increased by FHD treatment (Fig. 7C). The expression of OXPHOS complex in primary cultured brown adipocytes were determined by a western blot analysis, showing that the levels of OXPHOS complex 3 and 4 were significantly increased by FHD (Fig. 7D). These results

clearly indicate FHD can activate mitochondria by increasing mitochondrial biogenesis and OXPHOS system in primary cultured brown adipocytes.

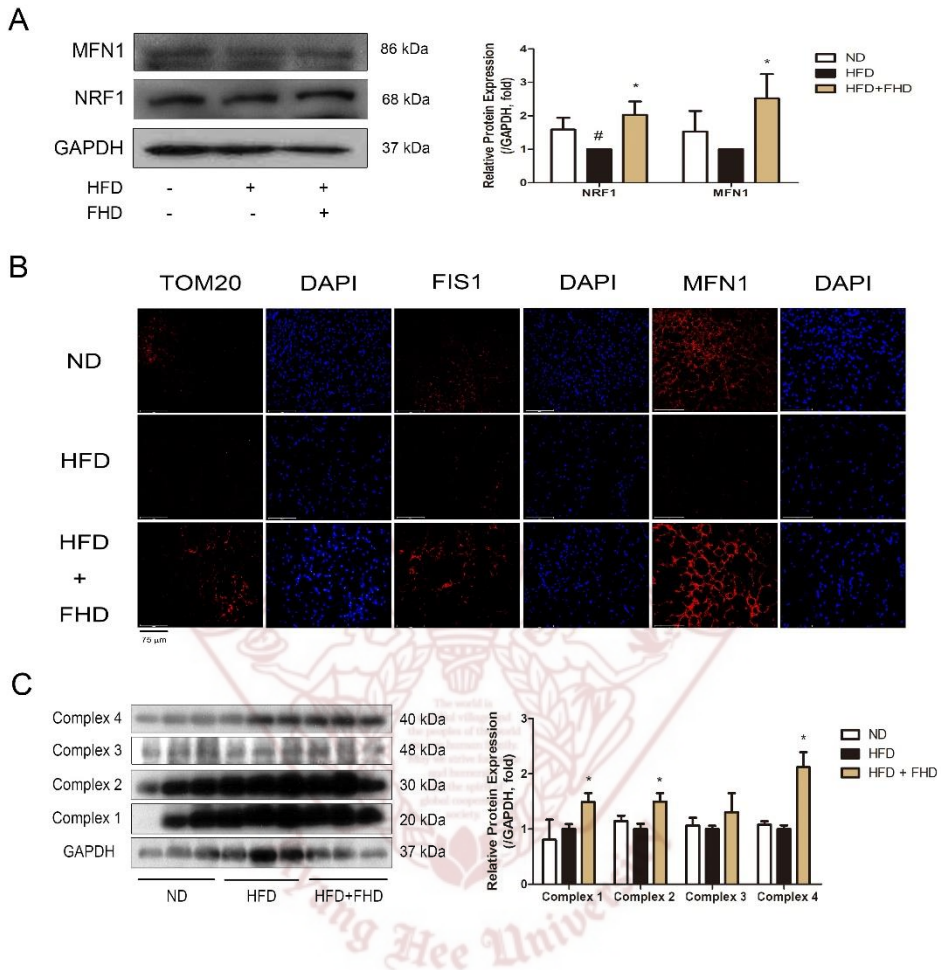

Figure 5. FHD increases mitochondria-related factors in BAT of HFD-induced obese C57BL/6 mice.

(A) Protein levels of NRF1 and MFN1 were analyzed by Western blot analysis in BAT. (B) Paraffin-embedded BAT sections from ND, HFD, and HFD+FHD mice were immunostained with antibodies for TOM20, MFN1 and FIS1, and counter-stained with DAPI for visualization of cell nucleus. (C) OXPHOS complex protein levels were analyzed by Western blot analysis in BAT. Results were expressed relative to GAPDH. All values are mean ± S.E.M. of data from three separate experiments. $^{\#}p < 0.05$, vs. ND-fed mice; $^{*}p < 0.05$, vs. HFD-fed mice. BAT, brown adipose tissue; HFD, high-fat diet; ND, normal diet.

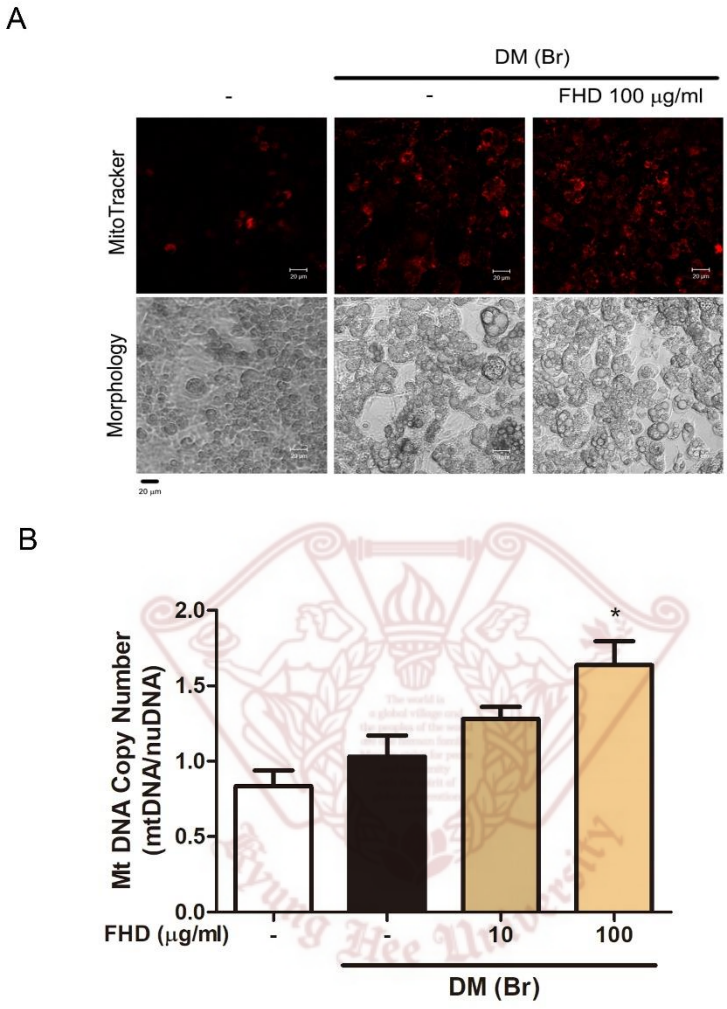

Figure 6. FHD increases mitochondria number in primary cultured brown adipocyte. (A) Mitochondrial abundance in primary cultured brown adipocytes was analyzed by MitoTracker Red staining. (B) Mitochondria DNA copy number in primary cultured brown adipocytes was assessed by real-time RT-PCR. Mitochondria DNA normalized by mouse nuclear DNA. All values are the means ± S.E.M. of three independent experiments. $^{\#}p < 0.05$, vs. DM-undifferentiated control cells; $^{*}p < 0.05$, vs. DM-differentiated control cells. DM, differentiated medium.

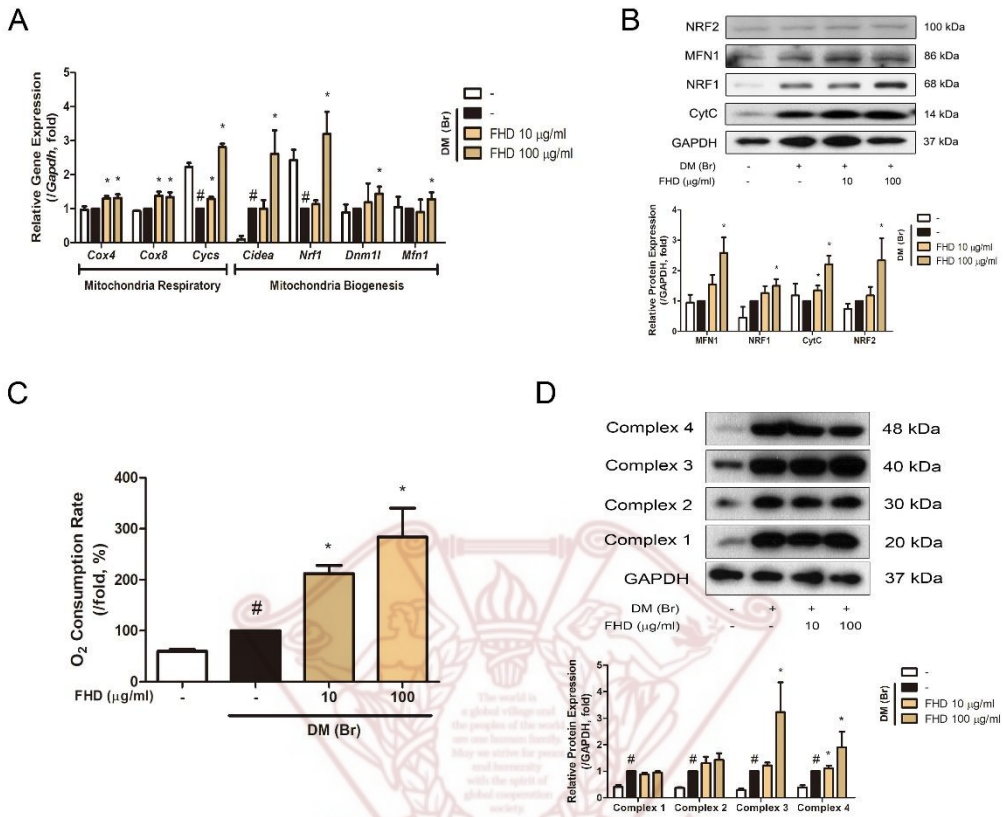

Figure 7. FHD activates mitochondria biogenesis in primary cultured brown adipocyte.

(A) The mRNA of *Cox4*, *Cox8*, *Nrf1*, *Cidea*, *Cycs*, *Dnm1l*, and *Mfn1* were analyzed by real-time RT-PCR. (B) Protein levels of NRF2, NRF1, MFN1, and CytC were analyzed by a Western blot analysis. (C) Oxygen consumption in primary cultured brown adipocytes was analyzed. (D) OXPHOS complex protein levels were analyzed by a Western blot analysis. Results were expressed relative to GAPDH. All values are mean ± S.E.M. of data from three separate experiments. $^{\#}p < 0.05$, vs. DM-undifferentiated control cells; $^{*}p < 0.05$, vs. DM-differentiated control cells. DM, differentiated medium.

4. FHD increases SIRT family in BAT of HFD-induced obese C57BL/6 mice and primary cultured brown adipocytes

From previous results, the author could confirm that FHD upregulated non-shivering thermogenesis, mitochondria biogenesis and activation in BAT and primary cultured brown adipocytes. For the next step, the mechanism of action of FHD on such effect was investigated. First, the author confirmed whether FHD altered the levels of SIRT family, which is well-known as a regulator of mitochondrial activation. As a result, FHD-treated group showed significantly higher levels of SIRT1 and SIRT3 than the control group, both in BAT of HFD-fed mice and primary cultured brown adipocytes (Fig. 8A-B). Next, the intracellular NAD expression level, one of the upstream regulators of the SIRT family, was confirmed in FHD-treated primary cultured brown adipocytes. The results showed that FHD clearly increased the intracellular total NAD level (Fig. 8C). To confirm the capability of FHD as an NAD regulator, FHD, NAD, and the NAD activator olaparib was treated respectively in primary cultured brown adipocytes. The expression level of intracellular total NAD was increased by both FHD and olaparib treatment, however the NAD-treated group did not show such change (Fig. 8D). Then, the SIRT1, SIRT3, PGC1α, and UCP1 protein were investigated after these treatments. FHD and olaparib showed similarly increased levels of SIRT1, SIRT3, PGC1α, and UCP1, with no statistical significance in UCP1 of the olaparib-treated cells (Fig. 8E). Through these results, the author could conclude that FHD can act as a strong inducer of intracellular NAD levels.

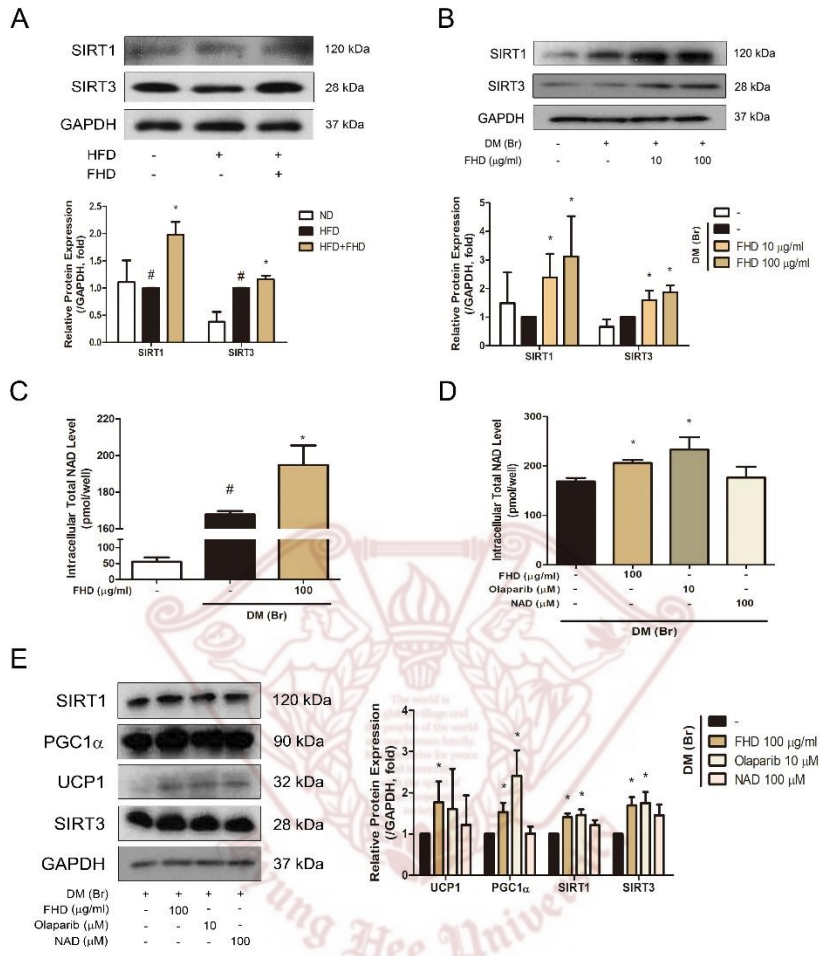

Figure 8. FHD activates SIRT family in BAT of HFD-induced obese C57BL/6 mice and primary cultured brown adipocytes.

(A) Protein levels of SIRT1 and SIRT3 were analyzed by a Western blot analysis in BAT of HFD-induced obese C57BL/6 mice (B) and primary cultured brown adipocytes. (C and D) Total intracellular NAD in primary cultured brown adipocytes was analyzed. (E) Protein levels of SIRT1, SIRT3, UCP1, and PGC1α were analyzed by a Western blot analysis. Results were expressed relative to GAPDH. All values are mean ± S.E.M. of data from three separate experiments. $^{\#}p < 0.05$, vs. DM-undifferentiated control cells or ND-fed mice; $^{*}p < 0.05$, vs. DM-differentiated control cells or HFD-fed mice. BAT, brown adipose tissue; HFD, high-fat diet; ND, normal diet.

Ⅳ. DISCUSSION

Adipose tissue consists of two types in humans: WAT and BAT. They have opposing roles in maintaining energy homeostasis [25]. In the past, BAT was believed to have a little physiological relevance since the tissue is present only in early childhood and disappears in adult. However, recently several studies have shown that BAT is located in the upper-chest and neck regions of adult humans and it is relevant [26, 27]. It has also been shown that BAT acts as an effector for non-shivering thermogenesis and lipid metabolism, with an increase in the density of BAT. Activating brown adipocyte differentiation increases energy expenditure by mitochondria and reduces weight gain [28], whereas decreased brown adipocyte differentiation is related to obesity and insulin resistance in humans [29]. Given these findings, BAT is currently considered to be a promising therapeutic target to resist obesity.

Recent studies have provided evidence on the capability of FHD in regulating hepatic diseases. For example, one study showed that FHD has a hepatoprotective effect by homeostatic regulation of inflammatory reaction [30]. Another study suggested FHD reduces the expression of lipogenesis and cholesterol synthesis-related proteins in fatty liver diseases [31]. Since excessive obesity is associated with hepatic disease, researchers argued that FHD has an obesity treatment effect. A previous study by Kim and colleauges previously also reported the inhibitory effect of FHD on adipogenesis in 3T3-L1 cells [20]. However the study was limited to an anti-adipogenic effect on white-differentiated adipocytes, and the anti-obese effect through the thermogenic activation is unknown.

Obesity is mainly due to the accumulation of lipids, changes in the morphology of adipose tissue can be used as a measure of obesity [32]. In the present study, FHD reduced body weight gain in HFD-fed mice, but food intake was the same in all groups. These results suggest FHD reduces weight gain regardless of diet. FHD increased serum HDL-C levels and decreased serum TC level. FHD also decreased the distribution of lipid droplets size in BAT of HFD-fed mice. From these results, the author believed that FHD

had an anti-obese activity in HFD-induced obese mice. The author then investigated whether FHD shows the anti-obesity effect through the thermogenic activity.

Brown adipocytes have an abundance of mitochondria, especially UCP1, which is located in the mitochondrial inner membrane, and is very important in the thermogenic action [33]. The thermogenic action of BAT consumes lipids without ATP production, and strongly depends on the activity of UCP1 [34]. PGC1α is also involved in thermogenic action with UCP1 [35]. FHD increased UCP1 and PGC1α levels in BAT of HFD-fed mice. The *in vivo* study was further supported by the in vitro experiments, indicating that FHD activates the differentiation of primary cultured brown adipocytes. FHD (10–100 μg/ml) did not cause significant cytotoxic effects and activates brown adipocyte differentiation, up-regulating UCP1 and PGC1α in primary cultured brown adipocytes. Furthermore, PRDM16, a transcription coregulator in development of brown adipocyte, as well as UCP1 and PGC1α also increased based on the dose of FHD in primary cultured brown adipocytes.

In addition, FHD increased the expression levels of mitochondria biogenesis-related proteins such as MFN1, NRF1, TOM20, and FIS1 in BAT of HFD-fed mice. FHD also induced mRNA expressions of the mitochondria biogenesis-related genes, including *Cox4, Cox8, Nrf1, Cidea, Cycs, Dnm1l,* and *Mfn1* in primary cultured brown adipocytes. MFN1, DLP1 and FIS1 is associated with mitochondria fusion and fission. An ongoing mitochondrial fusion and fission cycle allows mitochondrial functional and genetic complementation, and the proper distribution of newly synthesized mitochondria during cell division [36]. NRF is a transcription factor that activates nuclear genes such as the CytC whose products have a critical role in the proper mitochondrial function [37]. TOM20 is a complex of proteins found in the outer membrane of the mitochondria [38]. It allows movement of proteins through this barrier and into the intermembrane space of the mitochondrion [39]. Increased expression of TOM20 is a way to determine the amount of mitochondria. Mitochondrial content is also expressed as a copy number, which is maintained in a relatively safe range to meet the energy needs of cells to preserve normal physiological function [40]. As shown in TOM20/Mito-Tracker IF staining and real-time RT-PCR, FHD increased mitochondrial mass in both mitochondrial number and DNA in primary cultured brown adipocytes. These results indicate that FHD has a thermogenic

action and it induces thermogenesis through activating mitochondrial biogenesis in brown adipocytes.

These results showed that activation of OXPHOS complex as well as oxygen consumption was caused by FHD in BAT and primary cultured brown adipocytes. OXPHOS complex function inside the mitochondria, is the metabolic pathway in which cells use enzymes to oxidize nutrients, thereby releasing energy which is used to produce ATP [41, 42]. During oxidative phosphorylation, electrons are transferred from electron donors to electron acceptors such as oxygen, in redox reactions. These redox reactions release energy, which is used to form ATP [43]. Since ATP production through OXPHOS in mitochondria is essential for energy expenditure, the increase of OXPHOS system by FHD can be a potential evidence in anti-obesity effect of FHD. The OXPHOS complex not only play a role in energy expenditure but also contributes to the formation of electron gradients for the thermogenic activation by UCP1. Therefore, from the above mentioned results, we suggest that FHD activates the mitochondrial biogenesis and thermogenesis as well energy consumption via OXPHOS system and resulted in the regulation of body weight of obese mice.

Subsequently, we found that FHD activates mitochondrial biogenesis and thermogenesis in BAT and brown adipocytes. Then we determined which signal pathway FHD regulates and results in mitochondrial activation. The SIRT family is one of the notably increased thermogenic and mitochondrial factors [44, 45] . From our experiments, SIRT1 and SIRT3 were significantly increased by FHD in BAT of HFD-fed mice and primary cultured brown adipocytes. The SIRT family influences a wide range of cellular processes like aging, transcription, apoptosis, and inflammation, as well as energy efficiency and alertness during low-calorie situations [46, 47]. Also, the SIRT family increases the mitochondrial biogenesis in brown adipocytes [48]. Therefore, we suggest that FHD activates the mitochondrial biogenesis by increasing the SIRT1. The NAD+ levels are a central metabolic coenzyme and cosubstrate involved in cellular energy metabolism and energy production results in deacetylation/activation of PGC1α. In addition, increasing cellular NAD+ levels result in the activation of the SIRTs family [49, 50]. The intcellular NAD+ level is increased by FHD and olaparib, a NAD inducer, which

has been shown in previous study to induce browning of human primary white adipocytes [51]. However, NAD treatment did not induce any changes in brown adipocytes. Also, FHD and olaparib significantly increased the expression levels of SIRT1, SIRT3, PGC1α, and UCP1 proteins. From these facts the author can hypothesize that FHD increases intracellular NAD and induces SIRT family expression, thereby activating mitochondrial biogenesis and thermogenesis. Based on these results, further experiments will confirm that FHD increases thermogenesis and mitochondria biogenesis by increasing the SIRTs in brown adipocytes. Brief description of this study is summarized in Figure 9.

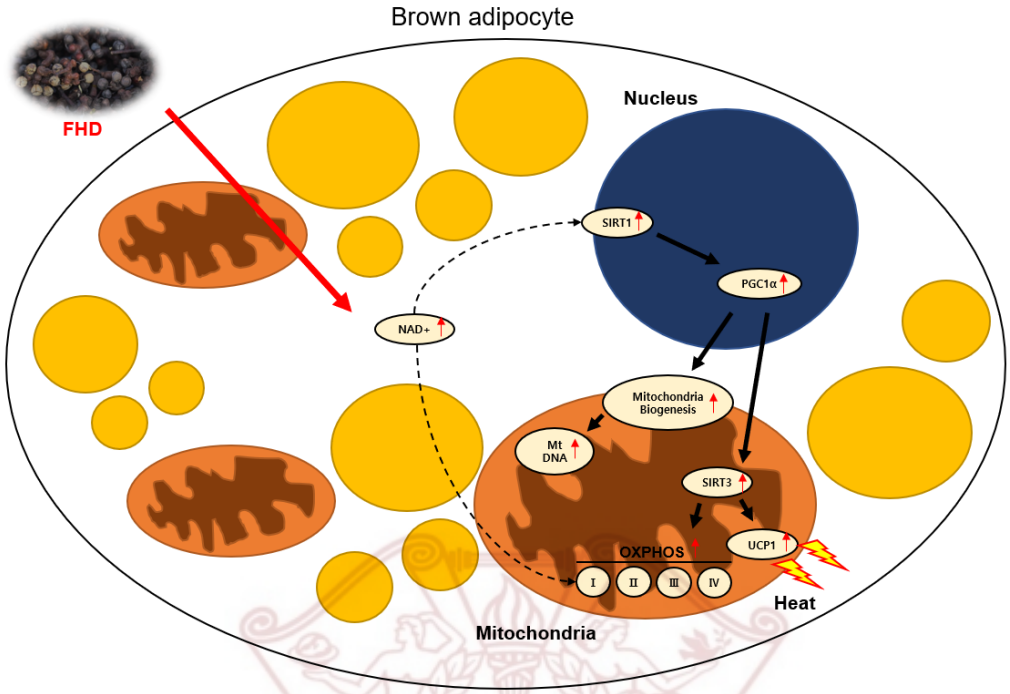

Figure 9. Diagrammatic visualization showing the contribution of FHD to the pharmacological pathways of obesity.

The fruits of *Hovenia dulcis* Thunb (FHD) increases intracellular NAD level. Increased intracellular NAD level activates SIRT1, SIRT3, and OXPHOS. Generally, pharmacological activation of SIRT1 upregulates transcriptional regulator of *Ppargc1a* gene, which increases thermogenesis and mitochondria biogenesis. Also, SIRT3 activates uncoupling mitochondrial respiration. These results suggest that FHD stimulates intracellular NAD and SIRT family expression, increasing thermogenesis and mitochondria activity.

V. CONCLUSIONS

In summary, this study provides the important evidence that FHD exhibits anti-obesity potentiality in HFD-induced obese mice. This is attributable to the decreased body weight gain and the ameliorated plasma lipid profiles. It is likely that these anti-obesity effects of FHD result from at least the partially increased expression levels involved in thermogenesis via UCP1 and PGC1α and the mitochondria activation by SIRT and NAD. Our identification of FHD as a natural activator of thermogenic effect and brown adipocyte differentiation opens a new research direction for pharmacological agents affecting energy expenditure in obesity and other metabolic disturbances.

VI. REFERENCES

1. Cypess AM, Lehman S, Williams G, Tal I, Rodman D, Goldfine AB, et al. Identification and importance of brown adipose tissue in adult humans. The New England journal of medicine. 2009;360:1509-17.
2. van Marken Lichtenbelt WD, Vanhommerig JW, Smulders NM, Drossaerts JMAFL, Kemerink GJ, Bouvy ND, et al. Cold-activated brown adipose tissue in healthy men. The New England journal of medicine. 2009;360:1500-8.
3. Orava J, Nuutila P, Lidell ME, Oikonen V, Noponen T, Viljanen T, et al. Different metabolic responses of human brown adipose tissue to activation by cold and insulin. Cell metabolism. 2011;14:272-9.
4. Cypess AM, Weiner LS, Roberts-Toler C, Franquet Elía E, Kessler SH, Kahn PA, et al. Activation of human brown adipose tissue by a β3-adrenergic receptor agonist. Cell metabolism. 2015;21:33-8.
5. Camont L, Chapman MJ, Kontush A. Biological activities of HDL subpopulations and their relevance to cardiovascular disease. Trends in molecular medicine. 2011;17:594-603.
6. Goldberg IJ. Lipoprotein lipase and lipolysis: central roles in lipoprotein metabolism and atherogenesis. Journal of lipid research. 1996;37:693-707.
7. Klaus S. Functional differentiation of white and brown adipocytes. BioEssays : news and reviews in molecular, cellular and developmental biology. 1997;19:215-23.
8. Petrovic N, Walden TB, Shabalina IG, Timmons JA, Cannon B, Nedergaard J. Chronic peroxisome proliferator-activated receptor gamma (PPARgamma) activation of epididymally derived white adipocyte cultures reveals a population of thermogenically competent, UCP1-containing adipocytes molecularly distinct from classic brown adipocytes. The Journal of biological chemistry. 2010;285:7153-64.
9. Mozo J, Emre Y, Bouillaud F, Ricquier D, Criscuolo F. Thermoregulation: what role for UCPs in mammals and birds? Bioscience reports. 2005;25:227-49.

10. Chechi K, Nedergaard J, Richard D. Brown adipose tissue as an anti-obesity tissue in humans. Obesity reviews : an official journal of the International Association for the Study of Obesity. 2014;15:92-106.
11. Porter C. Quantification of UCP1 function in human brown adipose tissue. Adipocyte. 2017;6:167-74.
12. Logan DC. The mitochondrial compartment. Journal of experimental botany. 2006;57:1225-43.
13. Canto C, Menzies KJ, Auwerx J. NAD(+) Metabolism and the Control of Energy Homeostasis: A Balancing Act between Mitochondria and the Nucleus. Cell metabolism. 2015;22:31-53.
14. Bai P, Canto C, Brunyanszki A, Huber A, Szanto M, Cen Y, et al. PARP-2 regulates SIRT1 expression and whole-body energy expenditure. Cell metabolism. 2011;13:450-60.
15. Houtkooper RH, Pirinen E, Auwerx J. Sirtuins as regulators of metabolism and healthspan. Nature Reviews Molecular Cell Biology. 2012;13:225-38.
16. Schug TT, Li X. Sirtuin 1 in lipid metabolism and obesity. Annals of medicine. 2011;43:198-211.
17. Haigis MC, Sinclair DA. Mammalian sirtuins: biological insights and disease relevance. Annual review of pathology. 2010;5:253-95.
18. Park JS, Kim IS, Shaheed Ur R, Na CS, Yoo HH. HPLC Determination of Bioactive Flavonoids in Hovenia dulcis Fruit Extracts. Journal of chromatographic science. 2016;54:130-5.
19. Ji Y, Chen S, Zhang K, Wang W. [Effects of Hovenia dulcis Thunb on blood sugar and hepatic glycogen in diabetic mice]. Zhong yao cai = Zhongyaocai = Journal of Chinese medicinal materials. 2002;25:190-1.
20. Kim HL, Sim JE, Choi HM, Choi IY, Jeong MY, Park J, et al. The AMPK pathway mediates an anti-adipogenic effect of fruits of Hovenia dulcis Thunb. Food & function. 2014;5:2961-8.
21. Jung Y, Park J, Kim HL, Sim JE, Youn DH, Kang J, et al. Vanillic acid attenuates obesity via activation of the AMPK pathway and thermogenic factors in vivo and

in vitro. FASEB journal : official publication of the Federation of American Societies for Experimental Biology. 2018;32:1388-402.

22. Jeong MY, Park J, Youn DH, Jung Y, Kang J, Lim S, et al. Albiflorin ameliorates obesity by inducing thermogenic genes via AMPK and PI3K/AKT in vivo and in vitro. Metabolism: clinical and experimental. 2017;73:85-99.
23. Cannon B, Nedergaard J. Brown adipose tissue: function and physiological significance. Physiol Rev. 2004;84:277-359.
24. Kalous KS, Wynia-Smith SL, Olp MD, Smith BC. Mechanism of Sirt1 NAD+-dependent Protein Deacetylase Inhibition by Cysteine S-Nitrosation. The Journal of biological chemistry. 2016;291:25398-410.
25. Rosen ED, Spiegelman BM. Adipocytes as regulators of energy balance and glucose homeostasis. Nature. 2006;444:847-53.
26. Cypess AM, Lehman S, Williams G, Tal I, Rodman D, Goldfine AB, et al. Identification and importance of brown adipose tissue in adult humans. The New England journal of medicine. 2009;360:1509-17.
27. van Marken Lichtenbelt WD, Vanhommerig JW, Smulders NM, Drossaerts JM, Kemerink GJ, Bouvy ND, et al. Cold-activated brown adipose tissue in healthy men. The New England journal of medicine. 2009;360:1500-8.
28. Tseng YH, Kokkotou E, Schulz TJ, Huang TL, Winnay JN, Taniguchi CM, et al. New role of bone morphogenetic protein 7 in brown adipogenesis and energy expenditure. Nature. 2008;454:1000-4.
29. Yang X, Enerback S, Smith U. Reduced expression of FOXC2 and brown adipogenic genes in human subjects with insulin resistance. Obesity research. 2003;11:1182-91.
30. Kim H, Kim YJ, Jeong HY, Kim JY, Choi EK, Chae SW, et al. A standardized extract of the fruit of Hovenia dulcis alleviated alcohol-induced hangover in healthy subjects with heterozygous ALDH2: A randomized, controlled, crossover trial. Journal of ethnopharmacology. 2017;209:167-74.
31. Kim B, Woo MJ, Park CS, Lee SH, Kim JS, Kim B, et al. Hovenia Dulcis Extract Reduces Lipid Accumulation in Oleic Acid-Induced Steatosis of Hep G2 Cells

via Activation of AMPK and PPARalpha/CPT-1 Pathway and in Acute Hyperlipidemia Mouse Model. Phytotherapy research : PTR. 2017;31:132-9.

32. Berry R, Church CD, Gericke MT, Jeffery E, Colman L, Rodeheffer MS. Imaging of adipose tissue. Methods in enzymology. 2014;537:47-73.
33. Fenzl A, Kiefer FW. Brown adipose tissue and thermogenesis. Hormone molecular biology and clinical investigation. 2014;19:25-37.
34. Brondani LA, Assmann TS, Duarte GC, Gross JL, Canani LH, Crispim D. The role of the uncoupling protein 1 (UCP1) on the development of obesity and type 2 diabetes mellitus. Arquivos brasileiros de endocrinologia e metabologia. 2012;56:215-25.
35. Ouellet V, Labbe SM, Blondin DP, Phoenix S, Guerin B, Haman F, et al. Brown adipose tissue oxidative metabolism contributes to energy expenditure during acute cold exposure in humans. The Journal of clinical investigation. 2012;122:545-52.
36. Seo AY, Joseph AM, Dutta D, Hwang JC, Aris JP, Leeuwenburgh C. New insights into the role of mitochondria in aging: mitochondrial dynamics and more. Journal of cell science. 2010;123:2533-42.
37. Scarpulla RC. Transcriptional activators and coactivators in the nuclear control of mitochondrial function in mammalian cells. Gene. 2002;286:81-9.
38. Saitoh T, Igura M, Obita T, Ose T, Kojima R, Maenaka K, et al. Tom20 recognizes mitochondrial presequences through dynamic equilibrium among multiple bound states. EMBO J. 2007;26:4777-87.
39. Tokatlidis K, Vial S, Luciano P, Vergnolle M, Clemence S. Membrane protein import in yeast mitochondria. Biochemical Society transactions. 2000;28:495-9.
40. [40] Clay Montier LL, Deng JJ, Bai Y. Number matters: control of mammalian mitochondrial DNA copy number. Journal of genetics and genomics = Yi chuan xue bao. 2009;36:125-31.
41. Mitchell P, Moyle J. Chemiosmotic Hypothesis of Oxidative Phosphorylation. Nature. 1967;213:137-9.

42. Formosa LE, Ryan MT. Mitochondrial OXPHOS complex assembly lines. Nature Cell Biology. 2018;20:511-3.
43. Cogliati S, Enriquez JA, Scorrano L. Mitochondrial Cristae: Where Beauty Meets Functionality. Trends in biochemical sciences. 2016;41:261-73.
44. Baskaran P, Krishnan V, Fettel K, Gao P, Zhu Z, Ren J, et al. TRPV1 activation counters diet-induced obesity through sirtuin-1 activation and PRDM-16 deacetylation in brown adipose tissue. Int J Obes (Lond). 2017;41:739-49.
45. Bagul PK, Katare PB, Bugga P, Dinda AK, Banerjee SK. SIRT-3 Modulation by Resveratrol Improves Mitochondrial Oxidative Phosphorylation in Diabetic Heart through Deacetylation of TFAM. Cells. 2018;7:235.
46. Preyat N, Leo O. Sirtuin deacylases: a molecular link between metabolism and immunity. Journal of leukocyte biology. 2013;93:669-80.
47. Satoh A, Brace CS, Ben-Josef G, West T, Wozniak DF, Holtzman DM, et al. SIRT1 promotes the central adaptive response to diet restriction through activation of the dorsomedial and lateral nuclei of the hypothalamus. The Journal of neuroscience : the official journal of the Society for Neuroscience. 2010;30:10220-32.
48. Shi T, Wang F, Stieren E, Tong Q. SIRT3, a mitochondrial sirtuin deacetylase, regulates mitochondrial function and thermogenesis in brown adipocytes. The Journal of biological chemistry. 2005;280:13560-7.
49. Hwang JH, Kim DW, Jo EJ, Kim YK, Jo YS, Park JH, et al. Pharmacological stimulation of NADH oxidation ameliorates obesity and related phenotypes in mice. Diabetes. 2009;58:965-74.
50. Li W, Sauve AA. NAD(+) content and its role in mitochondria. Methods in molecular biology (Clifton, NJ). 2015;1241:39-48.
51. Nagy L, Rauch B, Balla N, Ujlaki G, Kis G, Abdul-Rahman O, et al. Olaparib induces browning of in vitro cultures of human primary white adipocytes. Biochemical pharmacology. 2019;167:76-85.

국문 초록

헛개열매의 갈색지방 열발생 유도 및 작용기전에 관한 연구

송가희
기초한의과학과
경희대학교 대학원
지도교수: 엄재영

비만은 필요 이상의 에너지가 지질 형태로 축적되어 일어나서 생기는 의학적 상태를 말한다. 비만은 삶의 질을 떨어뜨릴 뿐 아니라, 다른 치명적인 질병의 위험을 증가시킬 수 있다. 지방 세포는 크게 갈색 지방과 백색 지방으로 나뉘며, 이 둘은 서로 반대되는 기능을 가진다. 백색 지방은 에너지를 지질로 저장하는 기능을 하며 백색 지방 내 과도한 지질의 축적은 비만의 원인이 된다. 반면, 갈색 지방은 백색 지방에 비해 많은 미토콘드리아를 함유하고 있어 미토콘리아 내막의 uncoupling protein 1 (UCP1)을 매개로 비 떨림 열 발생이라고 불리는 과정을 통해 저장된 에너지를 열의 형태로 방출한다. 갈색지방에서 일어나는 비 떨림 열 발생의 약리학적 활성화는 비만 치료를 위한 새로운 기전으로 주목받고 있다. 본 연구는 간 질환에 자주 사용되는 치료 약재인 헛개 열매(Fruit of *Hoveina dulcis* Thunb, FHD)가 갈색 지방 세포의 비 떨림 열 발생에 미치는 영향 및 그 상세기전을 규명하기 위해 진행되었다.

6주 간 FHD를 투여한 고지방식이 유도 비만 C57BL/6 쥐의 갈색 지방 조직과 일차 갈색 지방 세포를 이용하여 열 발생 및 그 작용 메커니즘에

미치는 FHD 의 효과를 조사한 결과, 열 발생과 관련된 인자인 UCP1 및 peroxisome proliferator activated receptor gamma-coactivator 1 alpha (PGC1α) 단백질의 발현이 증가되었다. 또한, FHD 의 처리는 sirtuin 3 (SIRT3) 와 sirtuin 1 (SIRT1)과 같은 미토콘드리아 활성 인자를 증가시켰을 뿐만 아니라 mitofusion 1 (MFN1) 및 nuclear respiratory factor 1 (NRF1) 등의 미토콘드리아 증식 인자의 발현 역시 유의미하게 증가시켰다. 또한, FHD 는 세포내에 존재하는 NAD 의 수준을 증가시켰으며, 이러한 NAD 의 증가는 FHD 에 의한 열발생을 활성화시키는 기전에 필수적으로 관여하는 것으로 보인다.

이러한 연구결과는 FHD 가 갈색지방에서 미토콘드리아의 활성화 및 비 떨림 열 발생을 증가시키는 효과를 가짐으로써 새로운 기전의 비만 치료제로 이용될 수 있는 잠재적인 가능성을 가짐을 시사한다.

핵심어: 헛개 열매; 비만; 갈색지방; 비 떨림 열 발생; 미토콘드리아